particle pulse is short enough, the duration of the moderated neutron pulses is roughly inversely proportional to the neutron speed.

These accelerator-driven pulsed sources are pulsed at frequencies of between 10 and 100 Hz.

There are two fundamental differences between a reactor and a pulsed source.

(1) *All* experiments at a pulsed source must be performed with time-of-flight techniques. The pulsed source produces neutrons in bursts of 1 to 50 μs duration, depending on the energy, spaced about 10 to 100 ms apart, so that the duty cycle is low but there is very high neutron intensity within each pulse. The time-of-flight technique makes it possible to exploit that high intensity. With the de Broglie relationship, for neutrons

$$\lambda\,(\text{Å}) = 0.3966\,t\,(\mu s)/L\,(\text{cm}),$$

where t is the flight time in μs and L is the total flight path in cm.

(2) The spectral characteristics of pulsed sources are somewhat different from reactors in that they have a much larger component of higher-energy (above 100 meV) neutrons than the thermal spectrum at reactors. The exploitation of this new energy regime accompanied by the short pulse duration is one of the great opportunities presented by spallation sources.

Fig. 4.4.1.2 illustrates the essential difference between experiments at a steady-state source (left panel) and a pulsed source (right panel). We confine the discussion here to diffraction. If the time over which useful information is gathered is equivalent to the full period of the source Δt (the case suggested by the lower-right figure), the *peak flux* of the pulsed source is the effective parameter to compare with the flux of the steady-state source. Often this is not the case, so one makes a comparison in terms of *time-averaged flux* (centre panel). For the pulsed source, this is lowered from the peak flux by the duty cycle, but with the time-of-flight method one uses a large interval of the spectrum (shaded area). For the steady-state source, the time-averaged flux is high, but only a small wavelength slice (stippled area) is used in the experiment. It is the *integrals* of the two areas which must be compared; for the pulsed sources now being designed, the integral is generally favourable compared with present-day reactors. Finally, one can see from the central panel that high-energy neutrons (100–1000 meV) are especially plentiful at the pulsed sources. These various features can be exploited in the design of different kinds of experiments at pulsed sources.

4.4.2. Beam-definition devices (By I. S. Anderson and O. Schärpf)

4.4.2.1. *Introduction*

Neutron scattering, when compared with X-ray scattering techniques developed on modern synchrotron sources, is flux limited, but the method remains unique in the resolution and range of energy and momentum space that can be covered. Furthermore, the neutron magnetic moment allows details of microscopic magnetism to be examined, and polarized neutrons can be exploited through their interaction with both nuclear and electron spins.

Owing to the low primary flux of neutrons, the beam definition devices that play the role of defining the beam conditions (direction, divergence, energy, polarization, *etc.*) have to be highly efficient. Progress in the development of such devices not only results in higher-intensity beams but also allows new techniques to be implemented.

The following sections give a (non-exhaustive) review of commonly used beam-definition devices. The reader should keep in mind the fact that neutron scattering experiments are typically carried out with large beams (1 to 50 cm^2) and divergences between 5 and 30 mrad.

4.4.2.2. *Collimators*

A collimator is perhaps the simplest neutron optical device and is used to define the direction and divergence of a neutron beam. The most rudimentary collimator consists of two slits or pinholes

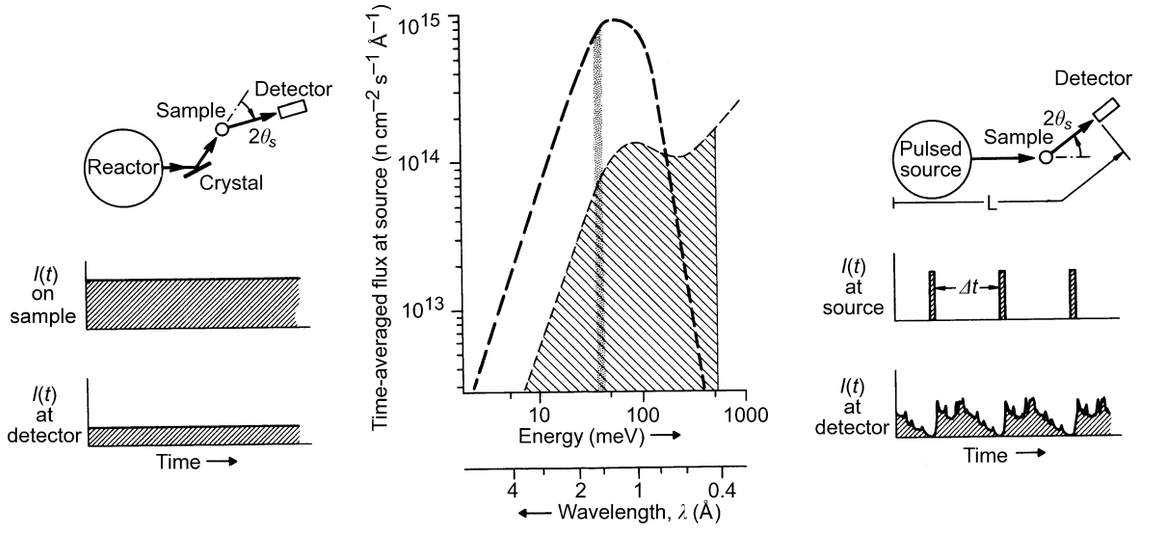

Fig. 4.4.1.2. Schematic diagram for performing diffraction experiments at steady-state and pulsed neutron sources. On the left we see the familiar monochromator crystal allowing a constant (in time) beam to fall on the sample (centre left), which then diffracts the beam through an angle $2\theta_s$ into the detector. The signal in the latter is also constant in time (lower left). On the right, the pulsed source allows a wide spectrum of neutrons to fall on the sample in sharp pulses separated by Δt (centre right). The neutrons are then diffracted by the sample through $2\theta_s$ and their time of arrival in the detector is analysed (lower right). The centre figure shows the time-averaged flux at the source. At a reactor, we make use of a narrow band of neutrons (heavy shading), here chosen with $\lambda = 1.5$ Å. At a pulsed source, we use a wide spectral band, here chosen from 0.4 to 3 Å and each one is identified by its time-of-flight. For the experimentalist, an important parameter is the integrated area of the two-shaded areas. Here they have been made identical.

Copyright © 2006 International Union of Crystallography

cut into an absorbing material and placed one at the beginning and one at the end of a collimating distance L. The maximum beam divergence that is transmitted with this configuration is

$$\alpha_{\max} = (a_1 + a_2)/L, \qquad (4.4.2.1)$$

where a_1 and a_2 are the widths of the slits or pinholes.

Such a device is normally used for small-angle scattering and reflectometry. In order to avoid parasitic scattering by reflection from slit edges, very thin sheets of a highly absorbing material, *e.g.* gadolinium foils, are used as the slit material. Sometimes wedge-formed cadmium plates are sufficient. In cases where a very precise edge is required, cleaved single-crystalline absorbers such as gallium gadolinium garnet (GGG) can be employed.

To avoid high intensity losses when the distances are large, sections of neutron guide can be introduced between the collimators, as in, for example, small-angle scattering instruments with variable collimation. In this case, for maximum intensity at a given resolution (divergence), the collimator length should be equal to the camera length, *i.e.* the sample–detector distance (Schmatz, Springer, Schelten & Ibel, 1974).

As can be seen from (4.4.2.1), the beam divergence from a simple slit or pinhole collimator depends on the aperture size. In order to collimate (in one dimension) a beam of large cross section within a reasonable distance L, Soller collimators, composed of a number of equidistant neutron absorbing blades, are used. To avoid losses, the blades must be as thin and as flat as possible. If their surfaces do not reflect neutrons, which can be achieved by using blades with rough surfaces or materials with a negative scattering length, such as foils of hydrogen-containing polymers (Mylar is commonly used) or paper coated with neutron-absorbing paint containing boron or gadolinium (Meister & Weckerman, 1973; Carlile, Hey & Mack, 1977), the angular dependence of the transmission function is close to the ideal triangular form, and transmissions of 96% of the theoretical value can be obtained with 10′ collimation. If the blades of the Soller collimator are coated with a material whose critical angle of reflection is equal to $\alpha_{\max}/2$ (for one particular wavelength), then a square angular transmission function is obtained instead of the normal triangular function, thus doubling the theoretical transmission (Meardon & Wroe, 1977).

Soller collimators are often used in combination with single-crystal monochromators to define the wavelength resolution of an instrument but the Soller geometry is only useful for one-dimensional collimation. For small-angle scattering applications, where two-dimensional collimation is required, a converging 'pepper pot' collimator can be used (Nunes, 1974; Glinka, Rowe & LaRock, 1986).

Cylindrical collimators with radial blades are sometimes used to reduce background scattering from the sample environment. This type of collimator is particularly useful with position-sensitive detectors and may be oscillated about the cylinder axis to reduce the shadowing effect of the blades (Wright, Berneron & Heathman, 1981).

4.4.2.3. *Crystal monochromators*

Bragg reflection from crystals is the most widely used method for selecting a well defined wavelength band from a white neutron beam. In order to obtain reasonable reflected intensities and to match the typical neutron beam divergences, crystals that reflect over an angular range of 0.2 to 0.5° are typically employed. Traditionally, mosaic crystals have been used in preference to perfect crystals, although reflection from a mosaic crystal gives rise to an increase in beam divergence with a concomitant broadening of the selected wavelength band. Thus, collimators are often used together with mosaic monochromators to define the initial and final divergences and therefore the wavelength spread.

Because of the beam broadening produced by mosaic crystals, it was soon recognised that elastically deformed perfect crystals and crystals with gradients in lattice spacings would be more suitable candidates for focusing applications since the deformation can be modified to optimize focusing for different experimental conditions (Maier-Leibnitz, 1969).

Perfect crystals are used commonly in high-energy-resolution backscattering instruments, interferometry and Bonse–Hart cameras for ultra-small-angle scattering (Bonse & Hart, 1965).

An ideal mosaic crystal is assumed to comprise an agglomerate of independently scattering domains or mosaic blocks that are more or less perfect, but small enough that primary extinction does not come into play, and the intensity reflected by each block may be calculated using the kinematic theory (Zachariasen, 1945; Sears, 1997). The orientation of the mosaic blocks is distributed inside a finite angle, called the mosaic spread, following a distribution that is normally assumed to be Gaussian. The ideal neutron mosaic monochromator is not an ideal mosaic crystal but rather a mosaic crystal that is sufficiently thick to obtain a high reflectivity. As the crystal thickness increases, however, secondary extinction becomes important and must be accounted for in the calculation of the reflectivity. The model normally used is that developed by Bacon & Lowde (1948), which takes into account strong secondary extinction and a correction factor for primary extinction (Freund, 1985). In this case, the mosaic spread (usually defined by neutron scatterers as the full width at half maximum of the reflectivity curve) is not an intrinsic crystal property, but increases with wavelength and crystal thickness and can become quite appreciable at longer wavelengths.

Ideal monochromator materials should have a large scattering-length density, low absorption, incoherent and inelastic cross sections, and should be available as large single crystals with a suitable defect concentration. Relevant parameters for some typical neutron monochromator crystals are given in Table 4.4.2.1.

In principle, higher reflectivities can be obtained in neutron monochromators that are designed to operate in reflection geometry, but, because reflection crystals must be very large when takeoff angles are small, transmission geometry may be used. In that case, the optimization of crystal thickness can only be achieved for a small wavelength range.

Nickel has the highest scattering-length density, but, since natural nickel comprises several isotopes, the incoherent cross section is quite high. Thus, isotopic ^{58}Ni crystals have been grown as neutron monochromators despite their expense. Beryllium, owing to its large scattering-length density and low incoherent and absorption cross sections, is also an excellent candidate for neutron monochromators, but the mosaic structure of beryllium is difficult to modify, and the availability of good-quality single crystals is limited (Mücklich & Petzow, 1993). These limitations may be overcome in the near future, however, by building composite monochromators from thin beryllium blades that have been plastically deformed (May, Klimanek & Magerl, 1995).

Pyrolytic graphite is a highly efficient neutron monochromator if only a medium resolution is required (the minimum mosaic spread is of the order of 0.4°), owing to high reflectivities, which may exceed 90% (Shapiro & Chesser, 1972), but its use is limited to wavelengths above 1.5Å, owing to the rather large d spacing of the 002 reflection. Whenever better resolution at

references